scientific reports

Check for updates

OPEN

Pharmacological inhibition of hypoxia induced acidosis employing a CAIX inhibitor sensitizes gemcitabine resistant PDAC cells

Jeevan Ghosalkar, Vinay Sonawane, Swati Achrekar & Kalpana Joshi✉

The poor prognosis of pancreatic ductal adenocarcinoma (PDAC) is attributed to tumor microenvironment driven by hypoxia regulated carbonic anhydrase IX. Our study elucidates the ability of Methazolamide, a CAIX inhibitor to sensitize resistant PDAC cells. The effect of Methazolamide alone and in combination with gemcitabine on proliferation, migration, tumor inhibition along with its impact on metastasis by influencing HIF-1α/PTEN/Glut1/Glut3 signalling through the expression of CAIX was assessed. Methazolamide induced cytotoxicity in several PDAC cells including patient derived with IC_{50} 0.7–4.09 mM and 0.29–2.56 mM in monolayer and clonogenic assays respectively. Methazolamide alone and in combination significantly downregulated hypoxia induced expression of HIF-1α and CAIX together with proliferation (Ki-67, Cyclin D1), invasion (Rac-1, Snail), stem cell (Oct-4, Sox-2), angiogenesis (VEGF), glycolysis (Glut1, Glut3) and apoptosis (Bax, Bc1-2 and PTEN) markers in MIA PaCa-2 and PANC-1 cells. In vivo study in PAXF 546L PDX model exhibited profound tumor growth inhibition with downregulation of CD34, Oct-4, Sox-2, C-myc, Nanog, Ki-67, and Rac-1 signalling. Considering inadequate availability of effective therapeutics and importance of CAIX in processes leading to aggressive behavior of PDAC, targeting it by using Methazolamide, a pre-approved drug in combination with gemcitabine represents promising therapeutic approach specifically in metastatic settings.

Keywords PDAC, Hypoxia, HIF-1α, Carbonic anhydrase, Methazolamide, Repurposing

Pancreatic cancer (PC), primarily represented by pancreatic ductal adenocarcinoma (PDAC) has one of the lowest survival rates and is third most common cause of cancer death in developed countries. It is estimated that 64,000 new diagnoses were made and more than 50,000 deaths (accounting for about 8.3% of all cancer death) were reported in 2023 for PC in the US. PC has a five-year survival rate of 12.5%, having one of the worst prognoses among all cancer types[1]. Importantly, it has been forecast that pancreatic cancer will surpass breast, prostate, and colorectal cancers as the leading cause of cancer-related death in the US by the year 2030[2]. Approximately 80% of patients present with unresectable (metastatic or locally advanced) disease with a median survival of 5 months[3]. The insolvability of this complex disease can be attributed to late diagnosis, scarcity of sensitive and specific biomarkers, early dissemination of metastases, and, notably, resistance to chemotherapy, radiotherapy, and currently available targeted therapies. Immunotherapy (IO) has been successful in numerous malignancies, but PDAC has been an exception. IO alone or in combination with cytotoxic chemotherapy and radiation among others, have been studied but have not shown meaningful clinical benefit[2]. Lack of effector cells in the tumor microenvironment (TME) combined with an immunosuppressive infiltrate, dense stroma impairing migration of effector cells, and immune checkpoint signaling are being considered as major mechanism of resistance to IO in PDAC. The only exception to this is FDA approval to pembrolizumab for the treatment of microsatellite instability—high (MSI-H) or deficient mismatch repair (dMMR) solid tumors including PDAC[2].

It is a well-known fact that PDACs are hypovascular and characterized by highly hypoxic TME, where the average oxygen level is 0.4% as opposed to 6.8% in the healthy pancreas[4]. This results in the up-regulation of hypoxia inducible factor 1 alpha (HIF-1α), which promotes the survival of cells under low-oxygen conditions

Discovery Biology Division, Cipla Ltd., LBS Marg, Vikhroli West, Mumbai 400083, India. ✉email: kalpana.joshi@cipla.com

but at the same time leading to production of acidic metabolites, the accumulation of which interrupts cellular function and viability. This in turn leads to the cancer cells upregulating a network of enzymes and transporters involved in pH regulation including the extracellular facing carbonic anhydrase IX (CAIX). CAIX is a cell surface metalloenzyme which catalyzes the reversible hydration of CO_2 to produce protons (H^+) and bicarbonate ($HCO3^-$), permitting tumor cells to survive exposure to acidosis. CAIX is overexpressed in response to hypoxia in many types of solid tumors including PC where it is driven by stabilization and constitutive activation of HIF-1α signaling because of mutation of the Von Hippel Lindau (VHL) tumor suppressor[5]. CAIX is often considered a surrogate marker of tumor hypoxia and is widely regarded as a prominent biomarker of poor patient prognosis for many solid cancers[6]. CAIX has also been identified as a key modulator of RAS-driven PDAC progression[7]. Since, CAIX is not widely expressed in normal human tissues, including pancreas[6] it is an attractive therapeutic target with a potential to enhance the efficiency of conventional therapies eventually leading to better prognosis. Studies have reported that blocking of CAIX overcomes ubiquitously encountered acidosis-promoted drug resistance, tumor cell invasion and metastasis[8].

Considering the critical role of CAIX in tumor growth and metastasis, in this study, we report repositioning of methazolamide (MZM) a synthetic derivative of sulphonamide and a known CAIX inhibitor against PC. MZM is currently approved for the treatment of increased intraocular pressure (IOP) in chronic open-angle glaucoma, secondary glaucoma and preoperatively in acute angle-closure glaucoma. The activity of MZM has also been exhibited pre-clinically against triple negative breast cancer, cervical cancer, alzheimer's disease, ankylosing spondylitis, diabetes, sepsis, mountain sickness and even against Covid-19[9–16]. Importantly, MZM shows a linear PK profile when administered orally and gets distributed throughout the body including the plasma, cerebrospinal fluid, aqueous humor, red blood cells, bile, and extracellular fluid. The mean steady-state plasma elimination half-life for MZM is approximately 14 h[17].

Here we demonstrate increased efficiency of combinatorial treatment consisting of CAIX inhibition through MZM and standard of care (SOC) gemcitabine (GEM). Persuasive evidence generated during this study suggest that MZM could be mechanistically suitable sensitizing agent inhibiting hypoxia induced expression of proliferation, invasion, stem cell, angiogenesis, glycolysis and apoptosis markers in dose and time dependent manner in both GEM sensitive and resistant cells. The data generated by us could provide insight into potentially active drug combinations for future treatment of PDAC.

Materials and methods

Cell lines and reagents

The pancreatic cancer cell line panel viz, AsPC-1, BxPC-3, Capan-2, HPAC, HuP-T3, MIA PaCa-2, PANC-1, Panc 10.05, PA-TU-8902 and SW 1990 were procured from ATCC (Rockville, MD, USA) or DSMZ (Braunschweig, Germany) and cultured in recommended complete media. Experimental methods on established patient derived xenograft (PDX) cells PAXF 546L, PAXF 1986L, PAXF 1998L, PAXF 2005L and PAXF 2059L were executed at Oncotest, Germany. The cells were maintained in a humidified chamber at 37 °C and 5% CO_2. All the compounds were dissolved in dimethyl sulfoxide (DMSO, #TC185, Sigma) at a concentration of 10 mM and diluted in culture medium immediately before use. MZM (#VIA-801223) and GEM (#SU0011214) were procured from Chemical Centre (Mumbai, India). Dulbecco's phosphate buffered saline (DPBS) without calcium and magnesium (#14025092), DMEM (#10566016) and FBS (#26140079) were purchased from Gibco, MA, USA. Lookout mycoplasma PCR kit (#MP0035), IMDM (#21980), RIPA buffer (#RO278) and PMS (#P9625) were from Sigma, MO, USA while 96-well flat-bottomed white polystyrene plates (#3912) were from Corning, NY, USA and MTS reagent (#G111) was procured from Promega, MA, USA.

In vitro cytotoxicity in 2D cell monolayer

In vitro anti-tumor activity of MZM was evaluated in a panel of pancreatic cell lines using Cell Titer-Blue® (#G8081, Promega, MA, USA) cell viability assay as per Joshi et al[18]. Cells were seeded in 96 well-plates (6000–20,000 cells/well), kept at 37 °C at 5% CO_2. Post 24 h incubation, MZM was added in the wells at indicated concentrations in triplicate for 24–72 h. After incubation, spent media was replaced with 100 µL fresh media and 20 µL Cell Titer-Blue reagent was added to the wells. Cells were incubated for ~ 4 h and relative fluorescence (RFU) was measured at Ex/Em:531/615 using Enspire Multimode Plate Reader (Perkin Elmer, USA). The results were calculated as % T/C over control. Half-inhibitory concentration (IC_{50}) values were computed with the help of GraphPad Prism using 4-parameter sigmoidal non-linear curve.

Ex vivo 3D cytotoxicity assay

MZM was also tested for its ability to inhibit growth of PDX or pancreatic cell lines in an anchorage independent semi-solid soft agar assay as per protocol established[19]. The assay plates were prepared by layering 50 µL of semi-solid agar containing 2500–10,000 cells/well in ultra-low attachment plates. A second layer of 100 µL medium was added followed by 24 h incubation. Post 24 h, test compound was added after serial dilution in IMDM. Cultures were incubated at 37 °C and 7.5% CO_2 in a humidified atmosphere for 8 or 13 days and monitored closely for colony growth using an inverted microscope. At the time of maximum colony formation, counts were measured with an automatic image analysis system (Cell Insight NXT, Thermo Scientific). Viable colonies were stained using Iodonitrotetrazolium Chloride.

Ex vivo combination studies

Cytotoxic effect of MZM and GEM was tested alone or in combination to inhibit anchorage-independent ex vivo tumor formation in semi-solid agar medium. Experiments were performed using PAXF 546L, PAXF 1986L, Capan-2 and MIA PaCa-2 cells in a 6 × 6 combination matrix. The effect of drug combination was evaluated using bliss independent analysis method to determine index of synergy[19].

Colony forming assay

Pancreatic cell lines MIA PaCa-2, PANC-1, AsPC-1, BxPC-3, Panc 10.05 and SW 1990 cells were seeded in 6-well plates (1000 cells/well) and incubated in complete media for 24 h. Cell were treated with MZM (0.5 and 1 mM) and GEM (400 nM) alone or in combination. After 48 h incubation, media containing drugs was replaced with fresh media and plates were further incubated for 7–10 days. The colonies formed were washed with PBS and were fixed with methanol: acetic acid mixture (1:6) for 30 mins. This was followed by washing and then by staining with 0.5% crystal violet for 30 mins. Visible colonies were quantified using Image J software (V1.52a)[18].

Wound healing assay

Pancreatic cell lines MIA PaCa-2, PANC-1, AsPC-1, BxPC-3, Panc 10.05 and SW 1990 cells were seeded in 24-well plates (1×10^6 cells/well) and incubated at 37 °C, 5% CO_2 for 24 h. Once 80–90% confluency was achieved, scratches were inflicted using micropipette tip in each well. To remove the detached cells, plates were washed using PBS and subsequently incubated with serum-free medium containing MZM (0.5 and 1 mM) and GEM (400 nM) alone or in combination for 24 h. Distance between the edges of the wound was measured 24 h post drug treatment. Images were captured at 10X magnification. Captured images were further quantified using Image J software to measure closure of the wound[19].

Protein expression studies

Protein expression was analyzed by Western blotting. MIA PaCa-2 and PANC-1 cells in two sets were seeded in 6-well plates (1×10^6 cells/well) and incubated at 37 °C, 5% CO_2 for 24 h. Post incubation, the media was replaced with fresh media and cells were treated with GEM (400 nM), MZM (0.5 and 1 mM) alone and combination. One set of plates were exposed to normoxia (21% O_2), and the second set exposed to hypoxia (1% O_2) for 24 h and 48 h. After 24 h and 48 h of incubation with compound the cells were harvested in 200 µL RIPA buffer to generate cell lysates. The samples generated were processed as per reported protocol[18]. In short, the total protein content in the lysates was quantified with the Pierce BCA protein assay kit (#23227). Proteins in cell lysates (around 5–50 µg) were separated on 7.5–12% SDS polyacrylamide gels and transferred by dry method to a PVDF/nitrocellulose membrane. The membranes were blocked for an hour at RT with 5% non-fatty milk (#1706404, Bio-Rad, Hercules, CA, USA,) solution in PBS containing 0.1% Tween (PBST). The membranes were incubated with various primary antibodies against different proteins viz, HIF-1α (#610658, BD Biosciences, England, UK), CAIX (#5649, Cell signaling, MA, USA), Ki-67 (#ab15580, Abcam, MA, USA), VEGF (#50661, Cell Signaling, MA, USA), Cyclin D1 (#2922, Cell Signaling, MA, USA) and GAPDH (#MA5-15738, Invitrogen, Canada) overnight followed by 3 washes with PBST. The membranes were then incubated with appropriate secondary antibodies (1:10,000 or 1:20,000) for 1 h at RT. After 3 washes with PBST, the immunoblots were developed using enhanced luminol-based chemiluminescent substrate (#WBLUF0100, Millipore, MA, USA) and the images were visualized using the ChemiDoc XRS system (Version 6.1, Bio-Rad, Hercules, CA, USA). The uncropped gel/blot images are provided as Supplementary 1.

Gene expression

MIA PaCa-2 and PANC-1 cells in two sets were seeded in 6-well plates (1×10^6 cells/well) and incubated at 37 °C, 5% CO_2 for 24 h. Post incubation, the media was replaced with fresh media and cells were treated with GEM (400 nM), MZM (0.5 and 1 mM) alone and combination. One set of plates were exposed to normoxia (21% O_2), and the second set exposed to hypoxia (1% O_2) for 3, 18 and 24 h before terminating treatment. The samples generated were processed as per protocol established[19]. RNA was extracted using Trizol (#15596026, Invitrogen, Carlsbad, Canada). The first-strand cDNA was synthesized (2 µg of total RNA) using Superscript III reverse transcriptase enzyme (#18080093, Invitrogen, Carlsbad, Canada) and oligo deoxythymidine (dT) as primers (Sigma Aldrich, India). Quantitative real time PCR (qRT-PCR) was performed using SYBR Green Supermix (#4309155, Thermofisher, MA, USA) as per the manufacturer's instructions. The relative changes in mRNA expression levels were assessed by $2^{-\Delta\Delta CT}$ method and changes in mRNA expression of target gene were normalized to that of GAPDH gene. The primer pairs of selected genes are listed in Supplementary 5.

In vivo efficacy

Female NMRI nu/nu mice (NMRI-Foxn1nu, ~6–8 wks.) from Charles River, Sulzfeld, Germany were housed in IVC cages with 12 h light and dark cycle, 55–75% relative humidity at 22–25 °C. Mice were implanted subcutaneously with ~30 mg PAXF 546L tumor fragment using Trocar needle in the right flank. All the animals were monitored for tumor growth. Once tumors attained the desired size (~100 mm^3), the mice were randomized and grouped (n = 8/group). CMC (0.5% in water, 10 mL/kg, P.O.) was used as vehicle control, MZM was dosed at 60 mg/kg/day P.O., GEM was administered at 50 mg/kg, I.V., while the combination group received MZM + GEM at 60 mg/kg, P.O. + 50 mg/kg/day I.V. (Table 3). Daily cage side observations were made for clinical signs. Body weight and tumor volume were recorded twice weekly throughout the experimental period. Mean tumor volume was calculated from tumor measurement data and Tumor Growth Inhibition (TGI) was calculated from tumor volume. Pharmacodynamics (PD) markers for mRNA transcript viz, *CD34, Oct-4, Sox-2, Nanog, C-myc, Ki-67, CD14, and Rac-1* were also evaluated from the tumor fragment. The study was conducted and approved by the Oncotest animal welfare body and the local authorities in accordance with German Animal Welfare act (Tierschutzgesetz) Oncotest (P441K, May 2016) and Animal Research: Reporting of In Vivo Experiments (ARRIVE) guidelines. Isoflurane was used as an anesthesia and euthanasia agent as per American Veterinary Medical Association (AVMA) 2020 Guidelines.

PDX cells	PAXF 1986L	PAXF 1998L	PAXF 2005L	PAXF 546L	PAXF 2059L
Passage	4N1	13N7	6N1	18N12	6
Histology	Adeno carcinoma	Adeno carcinoma	Adeno carcinoma	Adeno squamous carcinoma	Invasive ductal carcinoma
Differentiation	Moderate	Moderate	Poor	Good	Poor
Origin	Pancreas	Pancreas	Pancreas	Metastasis (Liver)	Pancreas
Stroma content	40%	5%	3.50%	13.33%	12.55%
Vascularization	High	High	High	High	Medium
Grading	Poor	Undifferentiated	Undifferentiated	Undifferentiated	Poor
Doubling time	8.8 days	4.3 days	5.2 days	5.7 days	5.4 days

Table 1. Panel of PDX cell lines with varying histopathological properties.

Cell line	Capan-2	Panc 10.05	SW 1990	BxPC-3	AsPC-1	MIA PaCa-2	PANC-1
Source	Primary	Primary	Metastasis, Spleen	Primary	Metastasis, ascites	Primary	Primary
HIF-1α	+	+	+ + +	+ +	+ +	+ + +	+ + +
CAIX	–	+ +	–	+ +	+ + + +	+ +	+ + +
CAXII	Low	–	+ +	+ + +	+	+ +	+ + +
VHL	W	W	W	W	W	W	W
KRAS	G12V	G12D	G12D	W	G12D	G12C	G12D
TP53	T125	I255N	P191del	Y220C	C135fs*35	R248W	R273H
CDKN2A	T18A19dup	–	Hom Del	M	L78Hfs*41	Hom Del	M
SMAD4	W	–	M	M	R100T	W	W
MAP2K4	W	W	W	M	M	W	M
FBXW7	W	W	W	W	M	W	W
Metabolic Phenotype	Slow Proliferating	Slow Proliferating	Glycolytic	Lipogenic	Slow Proliferating	Glycolytic	Glycolytic

Table 2. Panel of Pancreatic cell lines with varying degrees of genetic background (Hom Del - Homologous deletion; W - wildtype; M - mutated).

Statistical analysis

Statistical differences between the experimental groups were determined by One-way analysis of variance (ANOVA) followed by post hoc multiple variances using a Tukey test (IBM SPSS Statistics, V20). Efficacy of different drugs alone/combinations was expressed as modelled T/C value, which is the actual measured T/C values on a scale ranging from 0 to 1, where 1 corresponds to a T/C value of 100%. The bliss neutral value is the product of modelled T/C of individual drug concentrations. The difference between bliss neutral value and the modelled T/C value for the various combination was taken as bliss index. Bliss index is arranged on a scale ranging from − 1.0 to 1.0. Positive values (Bliss Index ≥ 0.15, blue) indicate synergy, negative values (Bliss Index ≤ − 0.15, red) indicate antagonism, and zero is the neutral value.

Results

In vitro cytotoxicity in PDX cells and Pancreatic cell lines in 2D and 3D model

The anti-tumor activity of MZM was evaluated in a panel of twelve pancreatic lines with diverse genetic background (Tables 1 and 2). These cell lines included PDX cells (PAXF 546L, PAXF 1986L, PAXF 1998L, PAXF 2005L and PAXF 2059L) and ATCC / DSMZ cell lines (MIA PaCa-2, PANC-1, BxPC-3, Capan-2, HUP-T3, HPAC, PA-TU-8902). All these cell lines were tested for IC_{50} determination in 2D monolayer and 3D anchorage-independent clonogenic assay. MZM showed absolute IC_{50} values of 1.58–3.81 mM in 2D assay and 0.29–0.86 mM in clonogenic assay in PDX cell lines. While IC_{50} for MZM in cell line-derived models were in the range of 0.7–4.09 mM in monolayer assays as compared to 0.29–2.56 mM in clonogenic assay (Fig. 1). Overall, MZM displayed a concentration-dependent activity in all twelve cell lines with a mean absolute IC_{50} value of 1.905 and 0.799 mM in 2D and 3D assay respectively (Fig. 2). The cytotoxicity response of MZM in anchorage-independent clonogenic assay was better in PDX cells.

Regulation of CAIX and HIF-1α

MZM being a CAIX inhibitor we initially looked at the pattern of basal level expression of CAIX and HIF-1α in MIA PaCa-2 and PANC-1 at different time points under normoxia and hypoxia both at transcript and protein levels. The levels of both HIF-1α and CAIX were indeed found to be upregulated under hypoxia as compared to normoxia (Fig. 2A and B).

Further, we also studied the ability of MZM to regulate the protein level expression of HIF-1α and CAIX. As shown in the data, MZM significantly downregulated the protein levels in a dose and time dependent manner in both the cell lines tested (Fig. 2C–F).

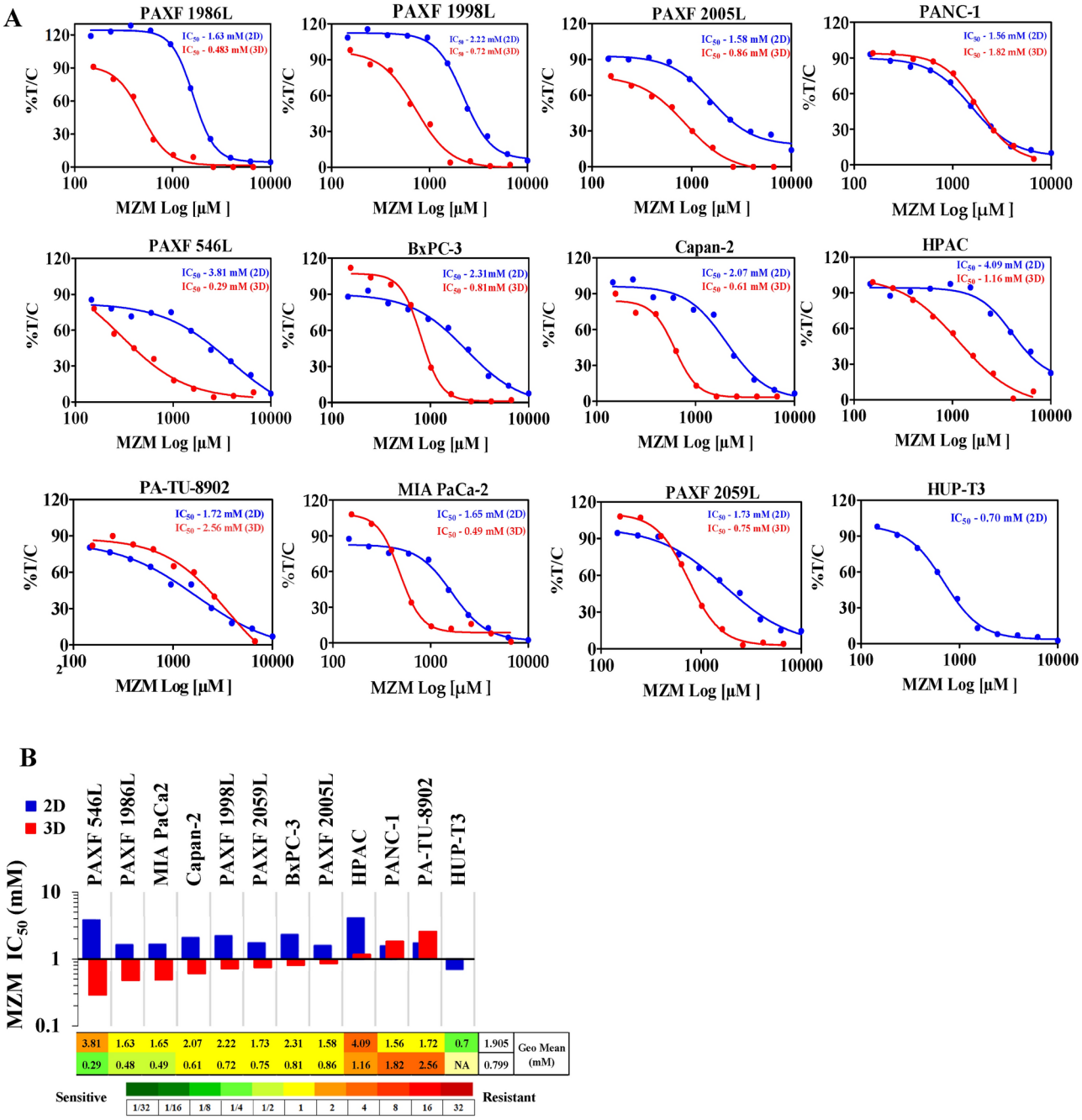

Fig. 1. Cytotoxicity of MZM in a panel of PDAC cell lines using 3D and 2D model. (**A**) In vitro and ex vivo cytotoxicity assay for MZM in panel of pancreatic cells at indicated concentrations. Ex vivo assay was performed in anchorage independent semi-solid soft agar 3D assay using PDX cell suspension or pancreatic cell lines. Cytotoxicity is expressed as % T/C as the ratio of treated by control. (**B**) Histograms represent rank order of IC_{50} values for MZM obtained for PDAC cells. The individual IC_{50} values are highlighted in colors ranging from dark green (≤ 1/32-fold geometric mean IC_{50}, corresponds to very potent compound activity or high tumor sensitivity) to dark red (≥ 32-fold geometric mean IC_{50}, corresponds to lack of compound activity or tumor resistance). The heat-map presentation, therefore, represents an anti-proliferative fingerprint profile of MZM.

MZM alone and in combination with GEM downregulates HIF-1α and CAIX

At the transcript level MZM alone as well as with GEM was able to significantly downregulate the expression of both HIF-1α and CAIX in MIA PaCa-2 and PANC-1 cells. Interestingly, the combination of MZM and GEM had a more pronounced effect on expression of HIF-1α and CAIX (Fig. 3A–D). Similarly, at the protein level too, the combination treatment exhibited higher efficacy in a time dependent manner under normoxia as well as hypoxia conditions in both MIA PaCa-2 and PANC-1 cells (Fig. 3E–H).

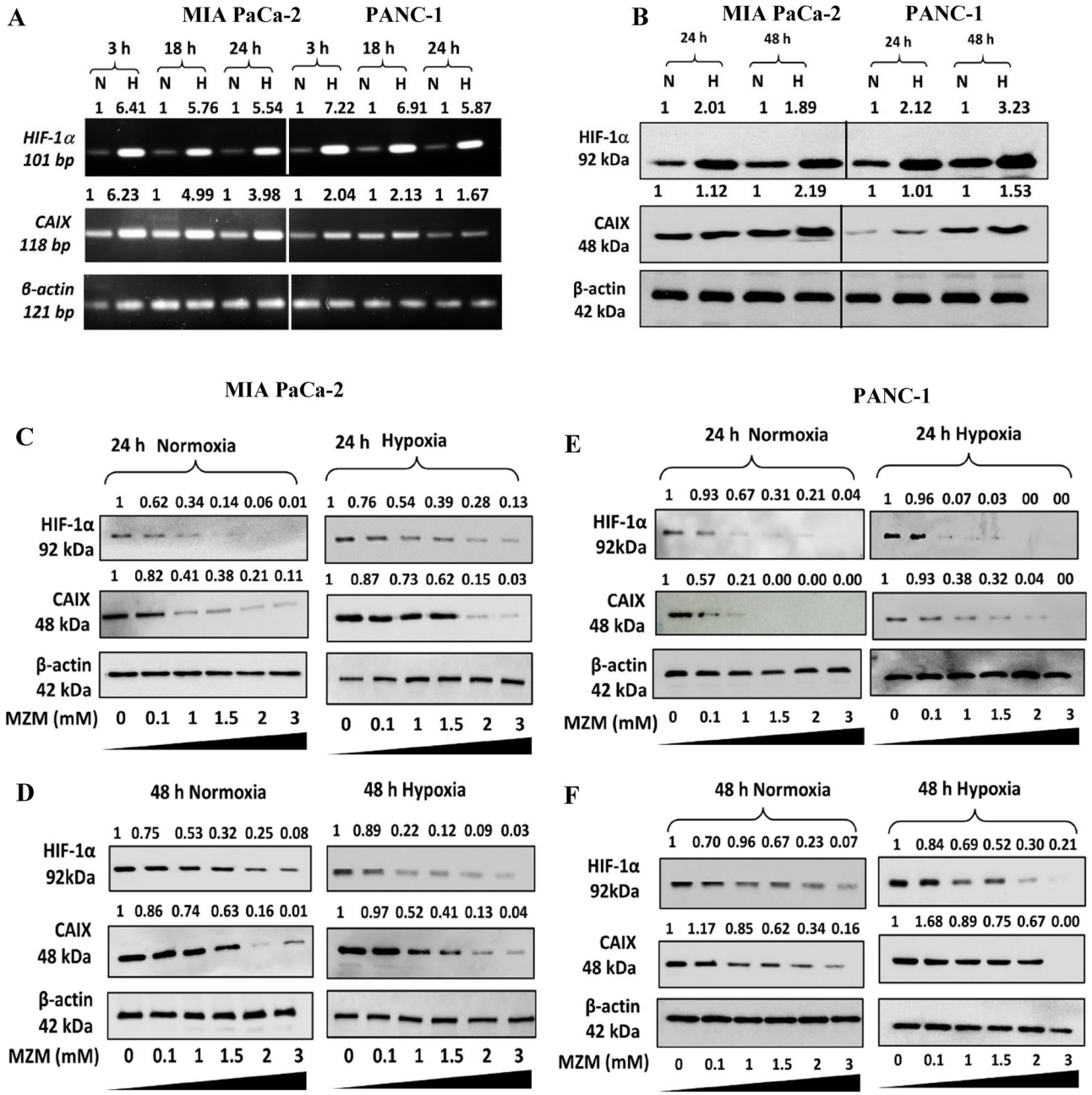

Fig. 2. Expression of HIF-1α and CAIX in MIA PaCa-2 and PANC-1 post MZM treatment. (**A**) Basal levels of mRNA transcript for *HIF-1α* and *CAIX* in MIA PaCa-2 and PANC-1 cells at 3, 18 and 24 h under hypoxia and normoxia. (**B**) Basal expression of HIF-1α and CAIX protein in MIA PaCa-2 and PANC-1 cells at 24 and 48 h. (**C**, **D**) Expression of HIF-1α and CAIX in MIA PaCa-2 cells treated with MZM at increasing concentrations (0.1–3 mM) for 24 and 48 h under hypoxia and normoxia. (**E**, **F**) Expression of HIF-1α and CAIX in PANC-1 cells treated with MZM at increasing concentrations (0.1–3 mM) for 24 and 48 h under hypoxia and normoxia.

Ex vivo combination studies

The ability of MZM to inhibit ex vivo colony formation as a single agent or in combination was examined in pancreatic tumor cell lines using 3D clonogenic assay in 6 × 6 combination matrix. MZM and GEM inhibited colony formation of pancreatic cells seeded in soft agar in dose dependent manner. This is also reflected in the matrix concentration, where activity of the different combinations was observed with increasing dose of both the compounds. Bliss independence analysis showed that combination of both the drugs produced additive effect in PAXF 1986L, PAXF 546L, Capan-2 and MIA PaCa-2 (Fig. 4A–D) as indicated in the color coding of the tiles in heatmap (additive effect: $-0.15 < BI < 0.15$). No antagonistic effects were recorded.

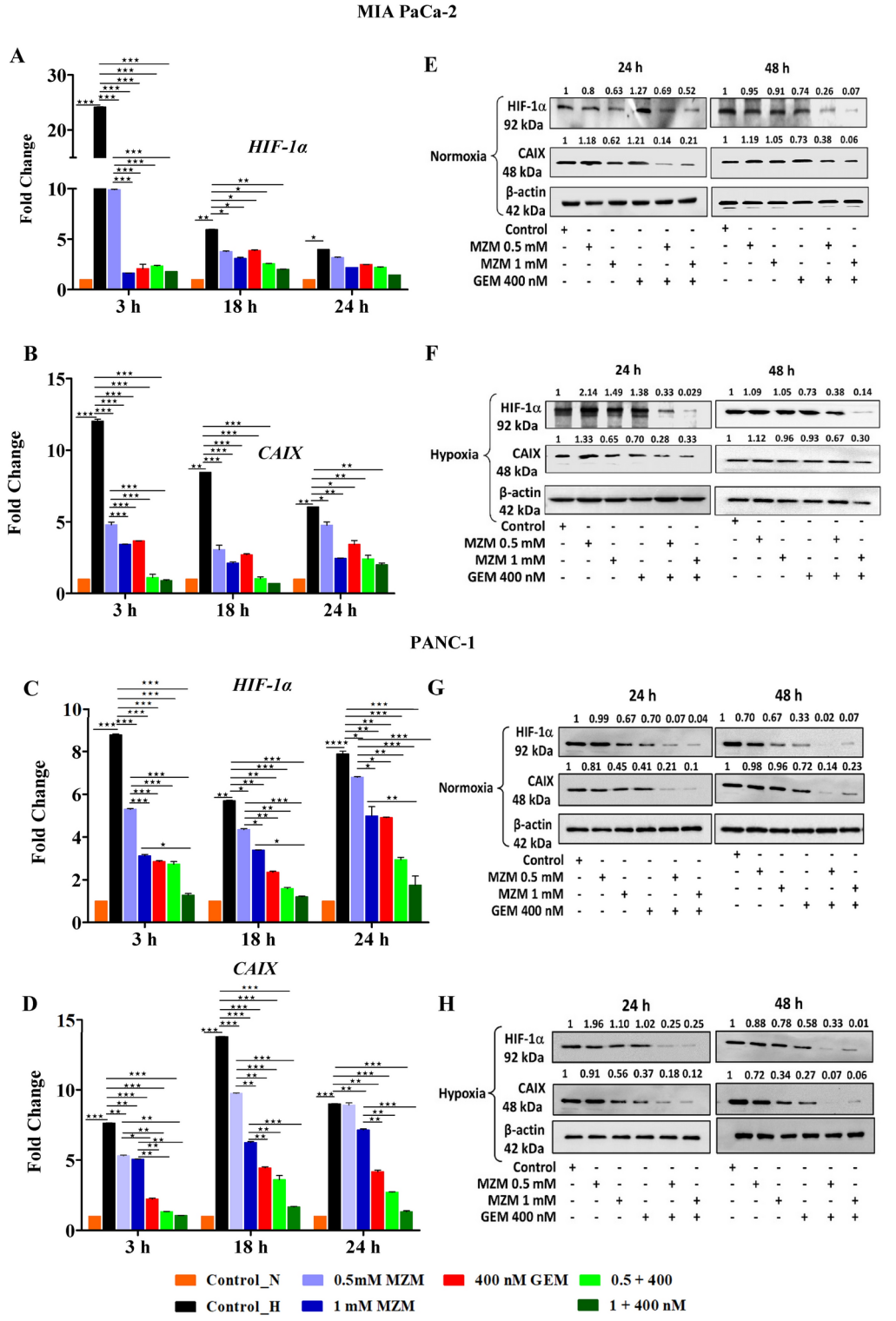

Fig. 3. Inhibition of HIF-1α and CAIX in PDAC cells. (**A–D**) Under hypoxia**,** mRNA transcripts levels of *HIF-1α* and *CAIX* in MIA PaCa-2 (**A** and **B**) and PANC-1 (**C** and **D**) post treatment with MZM alone or in combination with GEM. The relative expression of genes was calculated with the $2^{-\Delta\Delta Ct}$ method, using β-actin as housekeeping gene for normalization. Statistical differences between the groups were determined by one-way ANOVA and post hoc multiple variances using Tukey test. The statistically significant difference is represented as $^{*}p < 0.05$, $^{**}p < 0.01$ and $^{***}p < 0.001$ for control v/s specific group. (**E–H**) Western blot showing HIF-1α and CAIX protein expression levels in MIA PaCa-2 (**E** and **F**) and PANC-1 (**G** and **H**) post treatment with MZM alone or in combination with GEM (400 nM) at 24 and 48 h under normoxia (21% O_2) and hypoxia condition (1% O_2). Numbers on top indicate fold difference in expression which was determined after densitometry analysis using Image J software. β-actin was used as loading control.

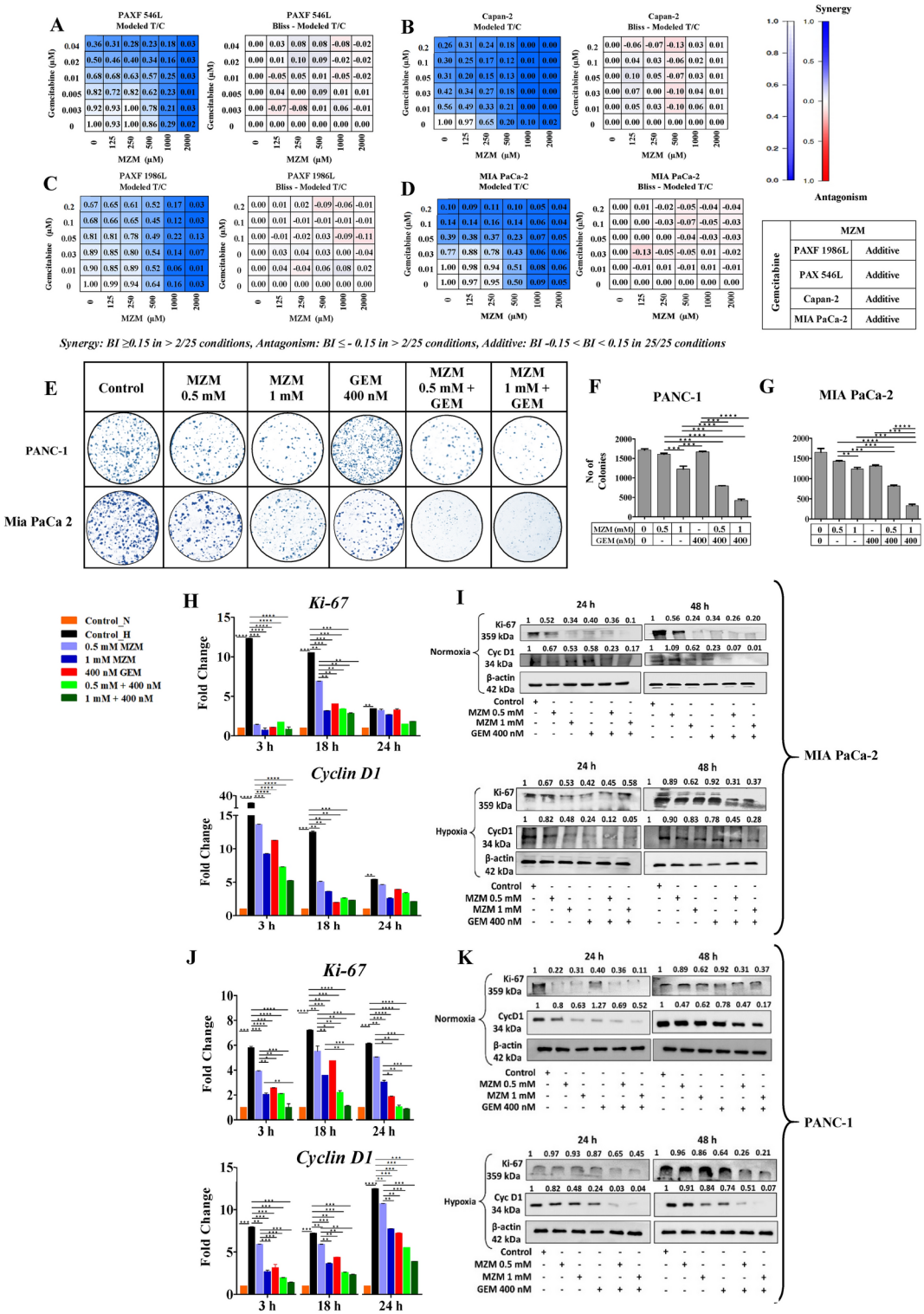

MZM with GEM affects the clonogenicity in pancreatic cells

The effect of MZM alone and in combination with GEM on MIA PaCa-2 and PANC-1 clonogenicity was analysed. Clonogenicity of MIA PaCa-2 and PANC-1 cells was observed to be gradually abolished by MZM both at lower and higher concentrations (0.5 and 1 mM). The combination of MZM and GEM drastically reduced cell growth as compared to vehicle control and drug alone (Fig. 4E, F and G). Similar effects were noted for AsPC-1, BxPC-3, Panc 10.05, and SW 1990 clonogenicity (Supplementary 2). Further, MZM alone was able to reduce the levels of important proliferation markers like Ki-67 and Cyclin D1 at transcript as well as protein levels under hypoxia conditions in both MIA PaCa-2 and PANC-1 cells (Fig. 4H–K). Similar observations were noted under normoxia conditions (Supplementary 4). Importantly, the reduction of these proliferation markers was more pronounced in combination of MZM and GEM treatment as compared to drug alone.

◀**Fig. 4**. Efficacy of MZM in combination with GEM in PDAC cells. Combination of MZM and GEM with 6 × 6 concentration matrix was evaluated using bliss index (BI) analysis in four PDAC cells viz, PAX 546L (**A**), PAXF 1186L (**B**) Capan-2 (**C**) MIA PaCa-2 (**D**). Bliss index is shown as the difference of the expected T/C value (Bliss neutral and the measured T/C value). Modelled T/C on a scale ranging from − 1.0 to 1.0. Positive values blue (Bliss Index ≥ 0.15) indicate synergy, negative values red (Bliss Index ≤ − 0.15) indicate antagonism, and zero (white) is the neutral value. **E,** Inhibition of anchorage dependent colony formation in MIA PaCa-2 and PANC-1 cells treated with MZM (0.5 and 1 mM) alone or in combination with GEM (400 nM). (**F–G**) Histograms represent quantification of stained colonies using Image J software. **H-J,** Histogram represents mRNA transcript of proliferation markers (*Ki-67* and *Cyclin D1)* in MIA PaCa-2 and PANC-1 cells at 3, 18 and 24 h on treatment with MZM alone or in combination with GEM. The relative expression of genes was calculated with the $2^{-\Delta\Delta Ct}$ method, using β-actin as housekeeping gene for normalization. (**I–K**) Expression of proliferation marker proteins (Ki-67 & Cyclin D1), in MIA PaCa-2 and PANC-1 cells post 24 and 48 h post treatment with MZM alone or in combination with GEM under normoxia and hypoxia. Numbers on top indicate fold difference in expression which was determined after densitometry analysis using Image J software. Statistical differences between the groups were determined by one-way ANOVA and post hoc multiple variances using Tukey test. The statistically significant difference is represented as $^{*}p < 0.05$, $^{**}p < 0.01$, $^{***}p < 0.001$ and $^{****}p < 0.0001$ for control v/s specific group.

MZM and its combination partner GEM restricts cell migration in pancreatic cells

The effect of MZM and it's combination partner GEM on MIA PaCa-2 and PANC-1 cell migration was evaluated by wound healing assay. MZM reduced cell migration in MIA PaCa-2 and PANC-1 cells at 24 h in a dose-dependent manner (Fig. 5A). The combination of MZM and GEM inhibited cell migration and wound closure more profoundly than drug alone (Fig. 5B, and C). Similar observation was noted for AsPC-1, BxPC-3, Panc 10.05**,** and SW 1990 (Supplementary 3). Simultaneously we also studied the effect of drug alone and in combination on the expression of crucial invasion markers viz, *Rac-1, Snail, Sox-2* in MIA PaCa-2 and PANC-1 under both normoxia (Supplementary 4) and hypoxia conditions at the transcript level. MZM alone was able to downregulate the expression of these markers in a dose and time dependent manner. Remarkably, the combination treatment was more efficacious in causing the downregulation as compared to drug alone (Fig. 5D and F). Furthermore, we also evaluated the ability of MZM to sensitize GEM in modulating its effect on VEGF as an angiogenesis marker. Data obtained indicates that combination of the drugs was more efficient in downregulating VEGF expression in both MIA PaCa-2 and PANC-1 cells under normoxia and hypoxia conditions (Fig. 5E and G).

MZM alone and in combination regulates apoptosis, stem cell and glucose metabolism markers

As discussed earlier, MZM alone and in combination with GEM could substantially down regulate the expression of CAIX and HIF-1α in MIA PaCa-2 and PANC-1 cells under both normoxia and hypoxia. Therefore, we went further and studied the effect of drugs on the differential expression of glycolysis markers *Glut1* and *Glut3*, stem cell marker *Oct-4* and apoptosis markers *Bax, Bcl-2* and *PTEN* at transcriptional level. The drug combination of MZM and GEM was able to cause significant decrease in hypoxia induced expression of *Glut1, Glut3, Oct-4, Bcl-2* and a substantial upregulation in the expression of *Bax* and *PTEN* in both cell lines tested (Fig. 6A and B).

In vivo efficacy

Anti-tumor efficacy of MZM was assessed in monotherapy and in combination with GEM in the PAXF 546L PDX tumor model. MZM alone caused a decrease in tumor volume up to 46%. While GEM alone showed 52% tumor regression. Importantly, combination of MZM with GEM led to sufficiently enhanced inhibition of tumor formation by 72%, clearly indicating superior anti-tumor efficacy as compared to drug alone (Fig. 7A and B). No adverse effects on body weights were observed indicating well tolerated dosage and schedule (Fig. 7C). Interestingly, PD studies also indicate inhibition of important proliferation, stemness and metastasis markers viz, *CD34, Oct-4, Sox-2, C-myc, Nanog, Ki-67*, and *Rac-1* (Fig. 7D).

Discussion

Pancreatic cancer has one of the lowest survival rates and is the third most common cause of cancer death in developing countries[3]. Numerous efforts are under way to alter the disease course to keep pace with the improved outcomes seen in other malignancies. Despite the ongoing labours survival for this disease is dismal. Immunotherapy, which has been efficacious in other cancers, is yet to see similar success in PC. Molecular profiling efforts have revealed that majority of PDAC patients harbored mutations (either germline or somatic) in *KRAS, TP53, CDKN2A, SMAD4, BRCA1, BRCA2*, and *PALB2* but none of them unfortunately have any therapeutic indication[2,20,21]. Recently, Larotrectinib and Entrectinib targeting the neurotrophic tyrosine receptor kinase (NTRK) gene were granted accelerated approval in 2018 and 2019 respectively on a tissue agnostic basis for unresectable or metastatic solid tumors where surgical resection is likely to result in severe morbidity, or for patients who have no satisfactory alternative treatments or that have progressed following treatment[22]. Of note is that the clinical trials conducted for Larotrectinib involved just one patient with pancreatic cancer, while Entrectinib had none[2].

Considering this abysmal scenario there is an urgent need for new and innovative treatment options for patients with this deadly disease. With high cost and long-time frame required for de novo drug development, drug repurposing represents a critical path to quickly identify potential treatments options for diseases with high unmet need[23]. The significance of drug repurposing is evident from the fact that this strategy was included in

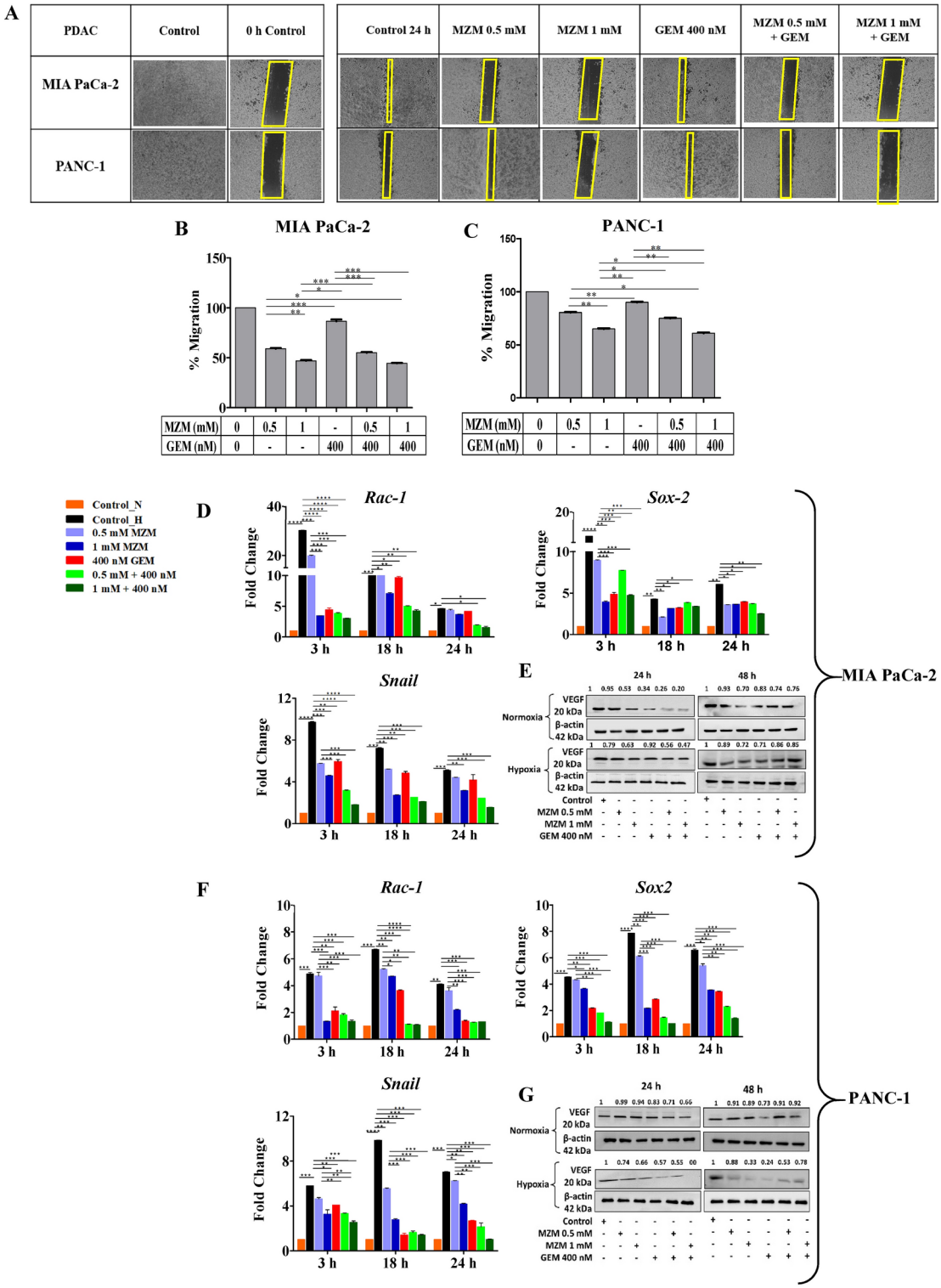

treatment guidelines (National Institutes of Health and Infectious Disease Society of America) for COVID-19 which demonstrates that drug repurposing "lived up to its promise of quickly leading to the development of effective COVID-19 therapeutics"[24].

In the present study we systematically investigated the efficacy of MZM against PC. MZM, a sulfonamide derivate and a potent inhibitor of carbonic anhydrases is indicated in the treatment of ocular conditions where reduction in IOP is likely to be of therapeutic benefit. The IC_{50} value of MZM against carbonic anhydrases ranges between 8 and 80 nM[8,25]. Many CAs are known to be associated with neoplastic growth, especially the hypoxia inducible CAIX, CAXII as well as the widely expressed CAII[26]. Considering its importance, currently, there are about ten on-going clinical trials for CAIX[27].

Furthermore, it has been apparent that extreme hypoxia and extracellular acidosis, the hallmark of PDAC, are major factors responsible for poor prognosis due to drug resistance and tumor metastasis. GEM, which is

◀**Fig. 5**. Wound healing assay for MZM alone (0.5 and 1 mM) and in combination with GEM (400 nM) in PDAC cells. (**A**) The migration and invasive potential in MIA PaCa-2 and PANC-1 post 24 h addition of compounds. Bar graphs show wound closure quantified by image J software for MIA PaCa-2 (**B**) and PANC-1 (**C**). One-way ANOVA was performed to analyse statistical significance. *($p < 0.05$), **($p < 0.001$), ***($p < 0.001$) and ****($p < 0.0001$). (**D** and **F**) Histogram represents modulation of proliferation markers (*Rac-1,*), stem cell markers (*Sox-2)* and EMT *(Snail)* in MIA PaCa-2 (**D**) and PANC-1 (**F**) cells at 3, 18 and 24 h after treatment with MZM alone or in combination with gemcitabine. The relative expression of genes was calculated with the $2^{-\Delta\Delta Ct}$ method, using beta actin as housekeeping gene for normalization. Statistical differences between the groups were determined by one-way ANOVA and post hoc multiple variance test using Tukey. The statistically significant difference is represented as *$p < 0.05$, **$p < 0.01$ ***$p < 0.001$ and ****$p < 0.0001$ for control v/s specific group. (**E–G**) Expression of VEGF protein in MIA PaCa-2 (**E**) and PANC-1 (**G**) cells post MZM treatment alone and in combination with GEM. Numbers on top indicate fold difference which was determined after densitometry analysis using Image J software.

still the SOC chemotherapeutic drug for PDAC has quite a low response rate (around 30%), and even lower in advanced cases. Chemoresistance develops rapidly mostly due to hypoxia induced EMT, glycolytic flux causing high cytidine pool that competes with GEM, activation of Hedgehog pathway which in turn leads to the expression of stem cell markers such as *CD44, Sox-2, Oct-4, Nanog*, and drug efflux proteins of the ATP binding cassette family. Thus, hypoxia not only increases resistance to GEM, but it also increases GEM-induced stemness[28]. Taking these factors into account we evaluated the efficacy of MZM alone and in combination with GEM under both normoxia and hypoxia conditions using multiple PDAC cell lines with varying genotypic permutations (Tables 1 and 2) both at transcript and protein levels using orthogonal pre-clinical models.

Our study distinctly signals significant anti-proliferative effect of MZM in PC and PDX cells alone as well as in combination with GEM. Interestingly, as per our observations the efficacy of MZM alone was more noticeable in the 3D model than 2D assays (geometric mean absolute IC_{50} value of 1.905 and 0.799 mM in 2D and 3D assay respectively). It is well known that 3D models more closely mimic the in vivo tumor morphology, cell phenotypes, heterogeneity, and the composition of TME making them more capable of capturing tumor cells' response to anti-cancer drugs and their penetration through the tumor tissue[18]. This observation of better efficacy in 3D model could be attributed to the presence of stromal component (Table 1) and better diffusivity of MZM. Additionally, MZM was also able to diminish the clonogenic capacity, downregulate proliferation and cell cycle markers viz, *Ki-67 and Cyclin D1* alone and in combination. This effect was more pronounced in the combination group.

Given the fact that tumor metastasis in PDAC is strongly associated with hypoxia and acidosis, we confirmed upregulation of HIF-1α and CAIX under hypoxic conditions in MIA PaCa-2 and PANC-1 cells. The increased expression was at both mRNA and protein levels. MZM subsequently down regulated them in dose and time dependent manner alone as well as in combination with GEM. Further, HIF-1α also directly activates the transcription of GLUTs, enzymes essential for tumor cell glycolysis, vascular endothelial growth factor (VEGF) and other proteins essential to cellular proliferation[29]. In addition, constitutively activated KRAS, present in more than 90% of PDAC also plays a key role in metabolic reprogramming, glycolytic switch and supports biomass synthesis (i.e. proteins, nucleic acids etc.) required for cancer cell proliferation[30]. Increased level of HIF-1α and activated KRAS is specifically associated with increased expression of *Glut1* and *Glut3* that allows the flux of glucose down its concentration gradient both in the presence of oxygen and under hypoxic conditions. MZM alone and significantly in combination with GEM down regulated the hypoxia induced transcript level expression of both *Glut1* and *Glut3* in MIA PaCa-2 and PANC-1 cells. Similarly, the combination was also found to be substantially effective in reducing the expression of VEGF. Remarkably, *PTEN* a known tumor suppressor and Bax, a pro-apoptotic factor and was significantly upregulated, while Bcl-2 was down regulated by MZM alone as well as in combination with GEM.

Since, tumor metastasis in PDAC is strongly associated with hypoxia and acidosis, we also studied inhibition of migration and invasion potential of PC cells by MZM alone and with GEM. Prominent inhibition was observed in MZM group at high concentration and in the combination group. Concurrently a significant decrease in crucial invasion markers viz, *Rac-1* and *Snail* was also noted in the combination treated groups. Additionally, hypoxia induced levels of *Sox-2* and *Oct-4*, known stemness, growth and invasion markers and important therapeutic target (FGFR/AKT/Sox-2 axis) in the fight against this very aggressive form of cancer[31,32] were found to be profoundly down regulated in combination treatment group. These in vitro results obtained by us were further corroborated in in vivo animal PD studies where the combination group exhibited highest anti-tumor efficacy and at the same time decreasing the expression levels of *CD34, Oct-4, Sox-2, Nanog, Ki-67, C-Myc and Rac-1*.

Current literature offers numerous studies that exhibit the clinical value of CAs and especially CAIX. Most data suggest that CAIX can serve as both biomarker and therapy target in diverse tumor types. Our present study clearly indicates the proficiency of MZM to regulate the expression of CAIX through management of HIF-1α. Notably, our data indicates that MZM successfully sensitizes PDAC cells with varying degree of genotype to GEM and aid in overcoming GEM related resistance. The multiple activities of MZM in cancer cells that modulate

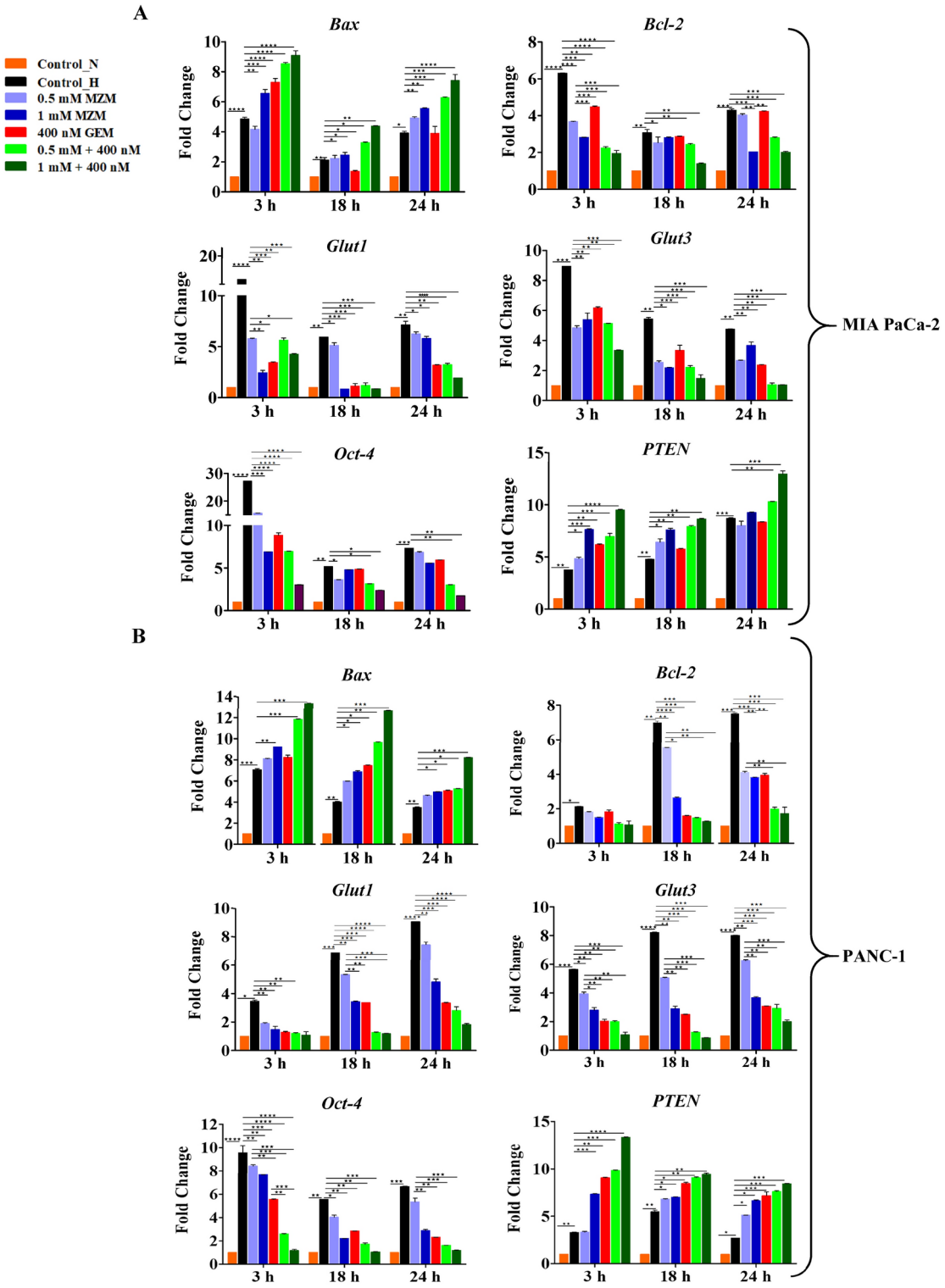

Fig. 6. Expression of apoptosis, glycolytic and stemness markers post treatment with MZM alone or in combination with GEM at indicated concentration. (**A**, **B**) Expression of mRNA transcript for *Bcl-2, Glut1, Glut3*, *Oct-4* and upregulation of *Bax and PTEN* in MIA PaCa-2 (**A**) and PANC-1 (**B**) respectively under hypoxia. The relative expression of genes was calculated with the $2^{-\Delta\Delta Ct}$ method, using β-actin as housekeeping gene for normalization. Statistical differences between the groups were determined by one-way ANOVA and post hoc multiple variances using Tukey test. The statistically significant difference is represented as $^{*}p < 0.05$, $^{**}p < 0.01$ $^{***}p < 0.001$ and $^{****}p < 0.0001$ for control v/s specific group. The differential regulation of markers at the transcript level needs to be confirmed at the translational level too.

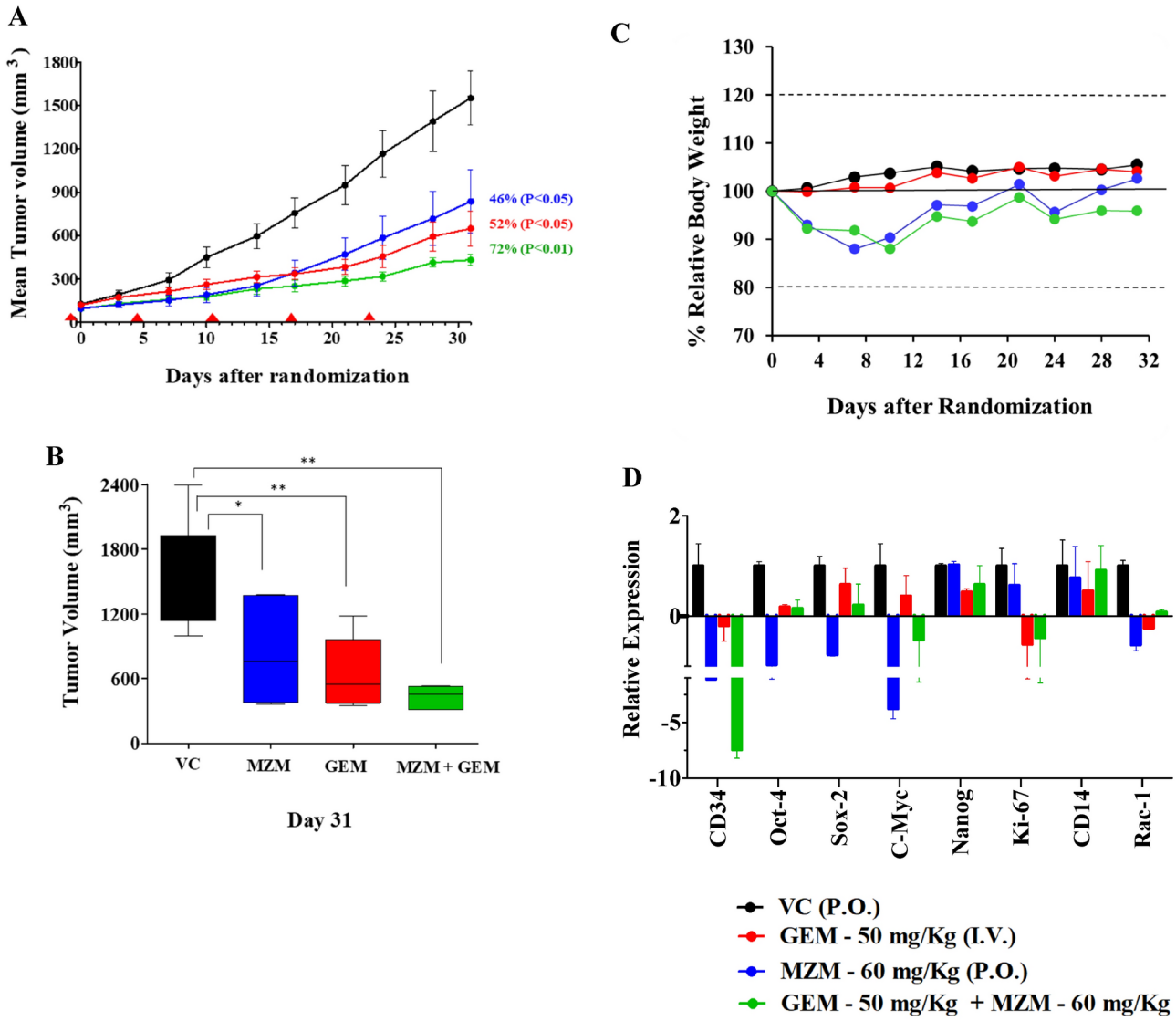

Fig. 7. In vivo efficacy of MZM in PAXF 546L PDX model. (**A**) Athymic nude mice were implanted with ~ 30 mg PAXF 546L tumor fragment using trocar needle in the flank region. Once tumor reached 100 mm^3, animals were randomized in different groups of MZM (60 mg/kg, P.O.) alone and in combination with GEM (50 mg/kg, I.V.). Tumor volume was measured every alternate day. (**B**) Histogram represents tumor volume on 31st day of the regimen. (**C**) Body weight of mice measured every alternate day during the treatment regimen. (**D**) qRT-PCR analysis in tumor samples obtained from xenograft model. The gene expression for the transcripts of *CD34, Oct-4, Sox-2, Nanog, C-Myc, Ki-67, CD14 and Rac-1* were studied in the groups of xenograft animals. *Gapdh* was taken as loading control.

Group - Therapy	Dose (mg/kg/day)	Schedule (Days)	Route
Group 1 - VC	0	1–11, 14–18, 21–25, 28–31	P.O.
Group 2 - GEM	50	1, 7, 14, 21, 28	I.V.
Group 3 - MZM	60	1–11, 14–18, 21–25, 28–31	P.O.
Group 4 - Combination GEM +	50 +	1, 7, 14, 21, 28	I.V. +
MZM	60	1–11, 14–18, 21–25, 28–31	P.O.

Table 3. Treatment summary that includes route of administration and days of dosing until day 31.

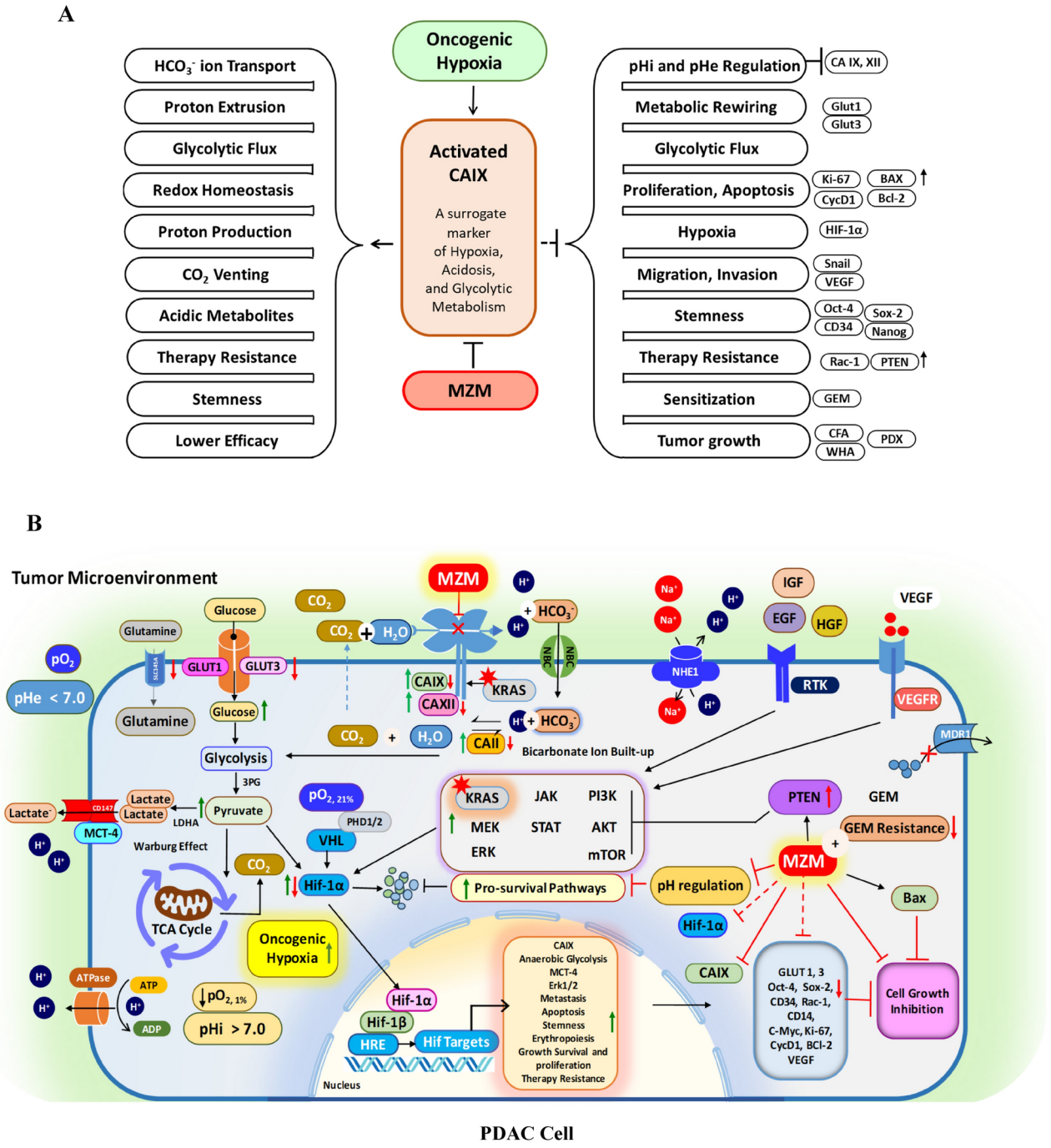

cellular pathway to induce growth inhibition, inhibition of invasion and stemness of PDAC cells impacting the crucial functions in PC have been summarized in Fig. 8A and B. Recently, an Open-label, multi-center, Phase 1b study to investigate the safety and tolerability of SLC-0111 (WBI-5111) a small molecule CA inhibitor in combination with GEM in metastatic PDAC subjects positive for CAIX has been initiated (NCT03450018) firming the significance of this combination approach. Interestingly, CAIX, has become a crucial target of choice for chimeric antigen receptor-T (CAR-T) cell therapy against glioblastoma and mccRCC[26,33]. Contrarywise, one of the greatest advantages of drug repurposing is reduced safety concerns, which often hamper the obtainment of valuable clinical candidates. In case of toxicity concerns metronomic approaches have often been employed to overcome such drawbacks considering risk versus benefit ratio of the treatment modality. Infact, metronomic chemotherapy (MCT) and drug repurposing are twenty-first century approaches developed to tackle the limitations of traditional chemotherapy[34]. Hence, we firmly believe that using MZM in combination with standard of care may hold promise for future clinical use in PC settings.

◀**Fig. 8**. (**A**) Inhibition of carbonic anhydrase IX as a surrogate marker of hypoxia, acidosis, and glycolytic metabolism by MZM in PC. Left side of figure indicates hypoxia related upregulation of CAIX and the related effects of this spike. The right of the figure indicates the inhibitory potential of MZM against all the markers studied and therefore all the pathways affected. *CFA, colony forming assay, WHA,wound healing assay; PDX, patient derived xenograft, GEM, Gemcitabine.* (**B**) Proposed cellular mechanism of action for MZM in PDAC cells. The illustration depicts proposed mechanism of MZM against carbonic anhydrase IX (CAIX) as a potential target in KRAS mutated pancreatic cancer. Under hypoxia, activated CAIX alters pH of intracellular milieu after intake of bicarbonate ions, generation of proton pool, increased uptake of glucose and accumulation of lactate. The altered pH favours stimulation of oncogenic signals by pro survival pathways which cater PC cells to proliferate, survive, invade, and metastasize under acidic environment. Pharmacological inhibition of CAIX by MZM modulates pericellular and intracellular activity owing to hypoxia, acidosis and glycolytic flux and further reduces tumor growth in GEM resistant PC cells. Abbreviations: MZM, Methazolamide; GEM, Gemcitabine, PDAC, Pancreatic ductal adenocarcinoma, NHE1, Sodium/proton exchanger 1; GLUT, Glucose transporter; MCT4, Monocarboxylate transporter 4; PTEN, Phosphatase and tensin homolog; NBC, Sodium bicarbonate cotransporter; IGF, Insulin growth factor; HGF, Hepatocyte growth factor; EGF, Epithelial growth factor; VEGF, Vascular endothelial growth factor; VEGFR, Vascular endothelial growth factor receptor; ATPase, Adenosine triphosphatase; HRE, Hypoxia response element; Hif-1α, Hypoxia inducible factor; MDR1, Multidrug resistance protein 1; RTK, Receptor tyrosine kinase; PHD1/2, Hypoxia-inducible factor prolyl hydroxylase 1/2; VHL, Von Hippel-Lindau Syndrome; LDHA, Lactate dehydrogenase A. Green upside arrow indicates upregulation under hypoxia. Red downside arrow indicates downregulation of effect mediated by MZM. pHe, extracellular pH; pHi, intracellular pH; red star indicates activated KRAS pathway.

Data availability

The datasets for all the supporting panels were uploaded in the supplementary files. Any additional data generated in this manuscript are available upon request from the corresponding author.

Received: 20 September 2024; Accepted: 6 March 2025
Published online: 14 May 2025

References

1. Cancer Stat Facts: Pancreatic Cancer. Accessed on April 2024; https://seer.cancer.gov/statfacts/html/pancreas.html
2. Roth, M.T, Cardin, D. B. & Berlin J. D. Recent advances in the treatment of pancreatic cancer. *F1000Res.* **9**, F1000 Faculty Rev-131. https://doi.org/10.12688/f1000research.21981.1 (2020).
3. Huynh, T. N. et al. The unmet needs of pancreatic cancer carers are associated with anxiety and depression in patients and carers. *Cancers* **15**(22), 5307. https://doi.org/10.3390/cancers15225307 (2023).
4. Estaras, M. & Gonzalez, A. Modulation of cell physiology under hypoxia in pancreatic cancer. *World J. Gastroenterol.* **27**, 4582–4602. https://doi.org/10.3748/wjg.v27.i28.4582 (2021).
5. Tatari, N. et al. Dual antigen T cell engagers targeting CA9 as an effective immunotherapeutic modality for targeting CA9 in solid tumors. *Front. Immunol.* **13**, 905768. https://doi.org/10.3389/fimmu.2022.905768 (2022).
6. Strapcova, S. et al. Clinical and pre-clinical evidence of carbonic anhydrase IX in pancreatic cancer and its high expression in pre-cancerous lesions. *Cancers* **12**, 2005. https://doi.org/10.3390/cancers12082005 (2020).
7. McDonald, P. C. et al. Regulation of pH by carbonic anhydrase 9 mediates survival of pancreatic cancer cells with activated KRAS in response to hypoxia. *Gastroenterology* **157**, 823–837. https://doi.org/10.1053/j.gastro.2019.05.004 (2019).
8. Kalinin, S. et al. Carbonic anhydrase IX inhibitors as candidates for combination therapy of solid tumors. *Int. J. Mol. Sci.* **2**, 13405. https://doi.org/10.3390/ijms222413405 (2021).
9. Paškevičiūtė, M. & Petrikaitė, V. Application of carbonic anhydrase inhibitors to increase the penetration of doxorubicin and its liposomal formulation into 2D and 3D triple negative breast cancer cell cultures. *Am. J. Cancer Res.* **10**, 1761–1769 (2020).
10. Improving Tumor Oxygenation in Cervical Cancer with Methazolamide. ClinicalTrials.gov ID NCT00257829, Sponsor, University of California, Irvine.
11. Fossati, S. et al. The carbonic anhydrase inhibitor methazolamide prevents amyloid beta-induced mitochondrial dysfunction and caspase activation protecting neuronal and glial cells in vitro and in the mouse brain. *Neurobiol. Dis.* **86**, 29–40. https://doi.org/10.1016/j.nbd.2015.11.006 (2016).
12. Sun, T. et al. Revealing mechanism of Methazolamide for treatment of ankylosing spondylitis based on network pharmacology and GSEA. *Sci. Rep.* **13**, 15370. https://doi.org/10.1038/s41598-023-42721-x (2023).
13. Simpson, R. W. et al. Efficacy and safety of oral methazolamide in patients with type 2 diabetes: A 24-week, placebo-controlled, double-blind study. *Diabetes Care.* **37**, 3121–3123. https://doi.org/10.2337/dc14-1038 (2014).
14. Rump, K. et al. Methazolamide reduces the AQP5 mRNA expression and immune cell migration—A new potential drug in sepsis therapy?. *Int. J. Mol. Sci.* **25**, 610. https://doi.org/10.3390/ijms25010610 (2024).
15. Teppema, L. J. et al. Influence of methazolamide on the human control of breathing: A comparison to acetazolamide. *Exp. Physiol.* **105**, 293–301. https://doi.org/10.1113/EP088058 (2020).
16. Li, Z. et al. Imatinib and methazolamide ameliorate COVID-19-induced metabolic complications via elevating ACE2 enzymatic activity and inhibiting viral entry. *Cell. Metab.* **34**, 424–440. https://doi.org/10.1016/j.cmet.2022.01.008 (2022).
17. Aref, A. A., Sayyad, F. E., Ayres, B. & Lee, R. K. Acute bilateral angle closure glaucoma induced by methazolamide. *Clin. Ophthalmol.* **7**, 279–282. https://doi.org/10.2147/OPTH.S41540 (2013).
18. Sonawane, V., Ghosalkar, J., Achrekar, S. & Joshi, K. Ketorolac modulates Rac-1/HIF-1α/DDX3/β-catenin signalling via a tumor suppressor prostate apoptosis response-4 (Par-4) in renal cell carcinoma. *Sci. Rep.* **13**, 5659. https://doi.org/10.1038/s41598-023-32627-z (2023).
19. Ghosalkar, J. et al. Prostate apoptosis response-4 (Par-4): A novel target in pyronaridine-induced apoptosis in glioblastoma (GBM) cells. *Cancers* **14**, 3198. https://doi.org/10.3390/cancers14133198 (2022).
20. Waddell, N. et al. Whole genomes redefine the mutational landscape of pancreatic cancer. *Nature* **518**, 495–501. https://doi.org/10.1038/nature14169 (2015).

21. Biankin, A. V. et al. Pancreatic cancer genomes reveal aberrations in axon guidance pathway genes. *Nature* **49**, 399–405. https://doi.org/10.1038/nature11547 (2012).
22. Gupta, M. et al. Targeting the NTRK fusion gene in pancreatic acinar cell carcinoma: A case report and review of the literature. *J. Natl. Compr. Canc. Netw.* **19**, 10–15. https://doi.org/10.6004/jnccn.2020.7641 (2021).
23. Zhang, Z. et al. Overcoming cancer therapeutic bottleneck by drug repurposing. *Signal Transduct. Target Ther.* **5**, 113. https://doi.org/10.1038/s41392-024-01808-1 (2020).
24. Greenblatt, W., Gupta, C. & Kao, J. Drug repurposing during the COVID-19 pandemic: Lessons for expediting drug development and access. *Health Affi.* **42**, 424–432. https://doi.org/10.1377/hlthaff.2022.01083 (2023).
25. Gudmundsdóttir, E. et al. Methazolamide 1% in cyclodextrin solution lowers IOP in human ocular hypertension. *Invest. Ophthalmol. Vis. Sci.* **41**, 3552–3554 (2000).
26. Haapasalo, J., Nordfors, K., Haapasalo, H. & Parkkila, S. The expression of carbonic anhydrases II, IX and XII in brain tumors. *Cancers* https://doi.org/10.3390/cancers12071723 (2020).
27. Singh, S., Lomelino, C. L., Mboge, M. Y., Frost, S. C. & McKenna, R. Cancer drug development of carbonic anhydrase inhibitors beyond the active site. *Molecules* **23**, 1045. https://doi.org/10.3390/molecules23051045 (2018).
28. Koltai, T. et al. Resistance to gemcitabine in pancreatic ductal adenocarcinoma: A physiopathologic and pharmacologic review. *Cancers* **14**, 2486. https://doi.org/10.3390/cancers14102486 (2022).
29. Cameron, M. E., Yakovenko, A. & Trevino, J. G. Glucose and lactate transport in pancreatic cancer: Glycolytic metabolism revisited. *J Oncol.* https://doi.org/10.1155/2018/6214838 (2018).
30. Cohen, R. et al. Targeting cancer cell metabolism in pancreatic adenocarcinoma. *Oncotarget* **6**, 16832–16847. https://doi.org/10.18632/oncotarget.4160 (2015).
31. Mirzaei, S. et al. SOX2 function in cancers: Association with growth, invasion, stemness and therapy response. *Biomed. Pharmacother.* **156**, 113860. https://doi.org/10.1016/j.biopha.2022.113860 (2022).
32. Zhang, Q., Han, Z., Zhu, Y., Chen, J. & Li, W. The role and specific mechanism of OCT4 in cancer stem cells: A review. *Int. J. Stem Cells* **3**, 312–325. https://doi.org/10.15283/ijsc20097 (2020).
33. Wang, Y. et al. Immune-restoring CAR-T cells display antitumor activity and reverse immunosuppressive TME in a humanized ccRCC mouse model. *iScience* **27**, 108879. https://doi.org/10.1016/j.isci.2024.108879 (2024).
34. Jan, N. et al. Metronomic chemotherapy and drug repurposing: A paradigm shift in oncology. *Heliyon* **10**(3), e24670. https://doi.org/10.1016/j.heliyon.2024.e24670 (2024).

Acknowledgements

Authors are thankful to Cipla Limited for supporting the scope of work.

Author contributions

JG, VS and KJ contributed for conceptualization, methodology, validation, and investigation. JG has contributed as a first author and SA, VS were involved in data curation and analysis, writing, and editing. SA produced key data for gene and protein expression studies. KJ supervised the overall project. All authors have read and agreed to the final version of the manuscript.

Declarations

Competing interests

The authors declare no competing interests.

Ethics approval

The study was conducted in accordance with German Animal Welfare act (Tierschutzgesetz) Oncotest (P441K and May 2016) for studies involving animals. And, in accordance with Animal Research: Reporting of In Vivo Experiments (ARRIVE) guidelines.

Additional information

Supplementary Information The online version contains supplementary material available at https://doi.org/10.1038/s41598-025-93388-5.

Correspondence and requests for materials should be addressed to K.J.